Annual Technical Report

Interface Engineering and Defect Control in Heteroepitaxial Growth of GaN

Supported under Grant #NOOO14-97-1-0859
Office of the Chief of Naval Research
Report for the Period of June 1997-May 1998

Robert J. Nemanich, Harald W. Ade and Robert F. Davis*
c/o Physics Department,
and
*Materials Science and Engineering Department
North Carolina State University
Campus Box 8202
Raleigh, NC 27695-8202

September 1998

REPORT DOCUMENTATION PAGE

Form Approved
OMB No. 0704-0188

1. AGENCY USE ONLY *(Leave blank)*	2. REPORT DATE	3. REPORT TYPE AND DATES COVERED
	September 12, 1998	Annual Technical Report June 1998

4. TITLE AND SUBTITLE
Interface Eneineering and Defect Control Heteroepitaxial Growth of GaN

5. FUNDING NUMBERS

6. AUTHOR(S)
Robert J. Nemanich, Harald W. Ade and Robert F. Davis

7. PERFORMING ORGANIZATION NAME(S) AND ADDRESS(ES)
North Carolina State University
Hillsborough Street
Raleigh, NC 27695-8202

8. PERFORMING ORGANIZATION REPORT NUMBER
NOOO14-97-1-0859

9. SPONSORING/MONITORING AGENCY NAMES(S) AND ADDRESS(ES)
Sponsoring: ONR, 800 N. Quincy, Arlington, VA 22217-5660
Monitoring: Administrative Contracting Officer, Office of Naval Research Regional Office Atlanta, 101 Marietta Tower, Suite 2805
101 Marietta Street, Atlanta, GA 30323-6145

10. SPONSORING/MONITORING AGENCY REPORT NUMBER

11. SUPPLEMENTARY NOTES

12a. DISTRIBUTION/AVAILABILITY STATEMENT
Approved for Public Release; Distribution Unlimited

12b. DISTRIBUTION CODE

13. ABSTRACT ***(Maximum 200 words)***

The technique of photo electron emission microscopy (PEEM) combined with UV free electron laser (UV-FEL) excitation has been employed for in situ studies of the dynamics of semiconductor interfaces. Wide bandgap semiconductors such as diamond, GaN and AlN exhibit a small or even negative electron affinity. The PEEM results show a shift of the photo threshold for in situ annealed diamond surfaces consistent with an increase in the electron affinity due to the desorption of hydrogen. The electron emission from an array of GaN emitters has been observed with PEEM and field emission electron microscopy (FEEM). Both measurements indicate nearly uniform emission from all of the elements of the array. The technique of PEEM with UV-FEL has been applied to explore a buried interface. The results display a buried Ti contact below an AlN layer. The dynamics of the formation of nanometer epitaxial islands on Si has been shown with PEEM. A unique aspect is that both ripening and coalescence processes are observed.

14. SUBJECT TERMS
Photo electron emission microscopy, PEEM, GaN, AlN interface dynamics

15. NUMBER OF PAGES
51

16. PRICE CODE

17. SECURITY CLASSIFICATION OF REPORT	18. SECURITY CLASSIFICATION OF THIS PAGE	19. SECURITY CLASSIFICATION OF ABSTRACT	20. LIMITATION OF ABSTRACT
UNCLAS	UNCLAS	UNCLAS	SAR

Table of Contents

I.	Characterization of Electron Emitting Surfaces of Diamond and III-V Nitrides *R. J. Nemanich, P. K. Baumann, M. C. Benjamin, S. L. English, J. D. Hartman, A. T. Sowers and B. L. Ward*	1
II.	Photoemission Electron Microscopy of buried TiAlN Interfaces *J. Hartman, S. English, W. Yang, H. Ade, R. Nemanich and R. Davis*	23
III.	Real-Time Observation of TI Silicide Epitaxial Islands Growth with the Photoelectron Emission Microscopy W. Yang, H. Ade, and R. J. Nemanich	35
IV.	Distribution list	51

CHARACTERIZATION OF ELECTRON EMITTING SURFACES OF DIAMOND AND III-V NITRIDES

R. J. Nemanich, P.K. Baumann, M.C. Benjamin, S.L. English, J.D. Hartman,

A.T. Sowers, B.L. Ward

Department of Physics and Department of Materials Science and Engineering

North Carolina State University, Raleigh, NC 27695-8202

Abstract

Wide bandgap semiconductors such as diamond and the diamond related materials of GaN and AlN, exhibit small or even negative electron affinities. Recent results have shown that surface treatments will modify the electron affinity of diamond to cause a negative electron affinity (NEA). For the III-V nitrides of GaN and AlN, results indicate a NEA for some surfaces of AlN and an electron affinity of 3.3 eV for GaN. Alloys of AlGaN exhibit a composition dependent electron affinity which trends to a value of zero at ~70% AlN. This study describes the characterization of these surfaces using UV photoemission spectroscopy (UPS), position dependent field emission and photo-electron emission microscopy (PEEM). Results are summarized which correlate the field emission from single crystal p-type (boron doped) diamond with various surface processes used to establish a NEA surface. The field emission threshold from the nitrogen doped samples is significantly higher than from p-type diamond, and in fact, most surfaces are severely damaged during the emission measurement. The PEEM technique, which combines aspects of UPS and field emission, images the emitted electrons allowing a true relation of the emission to the surface morphology. PEEM results are presented for both diamond and nitride surfaces.

Introduction

Electron emission from wide bandgap semiconductors offers the potential for cold cathode structures which would have a wide range of applications. Common semiconductors are based on sp^3 type bonding, and the incorporation of impurities can lead to p- or n-type doping characteristics. The discovery of a high quantum yield for photo-electron emission from diamond (111) surfaces indicated the potential for diamond as an electron emitter.[1] It was later concluded that the diamond (111) surface, when terminated with hydrogen exhibits a negative electron affinity.[2]

The property of a negative electron affinity will allow conduction band electrons to be freely emitted from a surface into vacuum without a barrier. Hence, the electron affinity of wide bandgap semiconductors has been the focus of many studies. However, the development of cold cathode devices will require emission without the assistance of light. Thus, field emission of wide bandgap semiconductors has also been studied as a validation of the materials properties required to fabricate cold cathode structures. While many investigators have employed field emission and photoemission to characterize surfaces, there have been significant differences in reports of similar materials. This study explores the characterization of electron emission characteristics of wide bandgap materials. In particular, photoemission results are summarized and correlated with field emission results. Moreover, we present photoelectron emission measurements which help display the point of origin of the electron emission.

The materials of diamond, boron nitride, SiC, Al-Ga-In nitrides and their alloys are often considered in the group of diamond-type materials because of their strong bonding leading to hard materials. These materials are stable for relatively high temperature operation, and they resist

defect formation and dopant diffusion. With these characteristics, they have been considered as a group for high power applications. With regards to field emission applications these same properties will be important for high current emission and a resistance to sputtering induced degradation.

While the ideal cold cathode material would exhibit a negative electron affinity as noted above, other properties are equally if not more important. The supply of electrons to the emitting surface will require a low resistance ohmic contact and transport of the electrons through the semiconducting material. To achieve these properties, n-type semiconducting characteristics may be required. Highly doped n-type material will allow low resistance contacts and provide electrons for transport through the material.

Field emission characterization of materials involves all of the attributes noted above. In fact, there are often many possible emission mechanisms so that it is sometimes impossible to determine the appropriate process for a single field emission measurement. In this study, we describe how photoemission and field emission techniques can be applied for the characterization of electron emission materials, and we summarize recent results on the diamond-type, hard, wide bandgap semiconductors. In a unique combination of the two techniques, we describe how photo-electron emission microscopy (PEEM) can be employed to relate the two processes and to determine the spatial characteristics of the electron emission.

Experimental

In this study measurements are presented for diamond and nitride surfaces. The samples include 3mm x 3mm x 0.25mm type IIb natural diamonds, boron or nitrogen doped microwave

plasma CVD diamond films grown on Si substrates, epitaxial AlGaN films, and Si doped GaN pyramid structures prepared by selective OMCVD growth processes. Details of the OMCVD growth processes have been presented elsewhere.[3]

For the photoemission measurements presented here, the spectra were excited with HeI radiation (21.2 eV), and the electrons were energy analyzed with a VSW 50mm mean radius hemispherical electron analyzer. All the measurements presented here were obtained for surface normal emission.[4]

The photoemission spectrum exhibits two aspects which indicate that the surface exhibits a negative electron affinity.[2, 4] The first is the presence of a strong sharp feature at low kinetic electron emission energies. The second attribute of a negative electron affinity at the surface is determined from the width of the spectrum. The width of the photoemission spectrum (W) can be related to the electron affinity (χ). The spectral width is obtained from a linear extrapolation of the emission onset edge to zero intensity at both the low kinetic energy cutoff and at the high kinetic energy end (reflecting the valence band maximum). The following relations apply for the two cases:

$$\chi = h\nu - E_g - W \text{ for a positive electron affinity} \qquad (1)$$

$$0 = h\nu - E_g - W \text{ for a negative electron affinity}$$

where E_g is the bandgap and $h\nu$ is the excitation energy. We stress that the photoemission measurements cannot be used to determine the energy position of the electron affinity for the NEA surface. Careful measurements of the width of the spectra are helpful in distinguishing whether the effect is direct emission of the electrons from conduction band states or excitons are

involved in the emission process. The effects of excitons have recently been reported by Bandis and Pate.[5]

Field emission measurements were obtained in an ultra-high vacuum (UHV) system with pressures typically < $1x10^{-8}$ Torr. A cylinder of molybdenum (3mm diameter) was selected as the anode for these measurements. The end of the cylinder was either polished flat or polished to a very high radius of curvature (typically > 5mm) to minimize edge effects. The anode is mounted on a stage that is coupled to a UHV stepper motor. One step of the motor corresponds to movement of the anode by 0.055μm. Current-voltage measurements are acquired with a computer controlled Keithley 237 Source Measure Unit (SMU). The SMU has the ability to simultaneously source a voltage and measure a current. A current limiting circuit is also included within the SMU so that no voltage is applied that causes the current to exceed $1x10^{-7}$A.

In any given measurement, a family of I-V curves is recorded with each curve corresponding to a different anode to sample spacing. Initially, the anode is positioned at some unknown distance above the sample. The stepper motor count is recorded and an I-V curve is collected. Next, the anode is moved closer to the sample by a known distance, and the cycle is repeated until at least 5-10 curves are collected. As expected, the current-voltage curves shift to lower voltage values with decreasing distance. Because of the nature of the Fowler-Nordheim I-V equation, the "turn-on" voltage or threshold voltage must be defined in terms of a specific current value. The voltage that results in a current value of 10nA was chosen to represent the threshold voltage for electron emission. This value was chosen because it is two orders of magnitude above the inherent noise current in our system. Next, each threshold voltage is plotted versus distance

relative to the first I-V curve, and as expected, the resulting graph was linear. Upon fitting the data to a straight line, the slope represents the average field for the threshold current emission. This method for determining the average field does not rely upon the absolute anode to sample spacing, but rather the change in distance of the anode with respect to the sample.

The PEEM measurements were obtained using a high resolution system from Elmitec. The sample holder supports a 5mm dia. substrate and employs electron beam assisted heating to greater than 1000 °C. The base pressure in the microscope is ~2 x 10^{-10} Torr. The Elmitec system employs an electromagnetic immersion lens, and has a lateral resolution of 10 nm. The sample is held a potential of -20,000V while the electron column is at ground potential. The field is applied by an anode (ground) positioned 2 mm from the sample surface (average field of 10 V/μm). The electrons are focused onto a microchannel plate and phosphor, and the image is recorded with a CCD camera outside the vacuum. Most measurements were obtained with UV light from a 100 W Hg lamp focused onto the sample. The light is incident on the sample at an average angle of 16 degrees. The high energy cutoff of the Hg lamp is ~ 5.1 eV. In some instances the spontaneous radiation from a free electron laser system was employed to obtain images. The light was obtained from the OK-4 UV free electron laser at the Duke University Free Electron Laser Laboratory.

In all experiments, separate images were also obtained with the light turned off. In some cases weak images were visible induced by only the applied field. These images are termed field electron emission microscopy (FEEM) images.

Results and Discussion

Photoemission of Diamond and Nitrides

The electron affinity of a semiconductor has been discussed in the same terms as the work function of a metal. The work function of a perfect metal surface is ascribed to aspects related to the electronic levels of the atoms involved in the material and the surface dipole. In the most fundamental terms, the surface dipole of a metal is related to the fact that the electron wave function extends beyond the potential defined by the atomic core. The electron density at the surface is balanced by an electron deficient region which results in a dipole. The field due to this dipole results in a potential which confines electrons in the material. This is a very simplified picture; in practice, it is not possible to calculate the surface dipole term, but it is possible to discuss how changing the surface changes the surface dipole. In general terms, the adsorption of an atomic species that is more electronegative than the surface atoms will increase the electron affinity while adsorption of a more electropositive species will decrease the electron affinity.

For a semiconductor, the actual electron orbitals and bonding configuration will also come to play in determining whether a change in the surface termination results in an increase or decrease in the electron affinity. For diamond it is now recognized that adsorbate free surfaces or oxygen termination of clean surfaces both result in a positive electron affinity while hydrogen termination results in a negative electron affinity.[4]

The results of an extensive UV photoemission study of surface preparation processes on type IIb diamond are summarized in Table 1.[6] Following prior studies it may be concluded that NEA surfaces are terminated with hydrogen while surfaces that exhibit a positive electron affinity are either oxygen terminated or adsorbate free. The initial diamond surfaces were

prepared with either a chromic acid etch or an electrochemical etch in water. For the (100) surface both processes have been shown to result in oxygen termination characterized by a positive electron affinity. The difference in the electron affinity apparently indicates differences in the bonding or surface termination. Annealing of these surfaces results in the observation of a negative electron affinity. We attribute this to desorption of oxygen which is replaced by hydrogen termination. We speculate that the hydrogen evolves from the bulk to the surface. After higher temperature annealing the hydrogen desorbs, and the adsorbate free surface exhibits a positive electron affinity. One interesting aspect is that the (111) surface is often observed to exhibit a NEA after the wet chemical treatment. We suggest that this surface is at least partially terminated with hydrogen. There are differences in the desorption temperature for the different surface orientations. For the (100) surface, oxygen is observed to completely desorb at ~900°C while for the (111) and (110) surfaces, the oxygen desorbs for annealing at 700°C or less. Similarly, The hydrogen is observed to evolve from the (100) surface after annealing at 1100°C, while annealing at 900 and 800 °C are required for H desorption of the (111) and (110) surfaces, respectively.

Since large crystals of the III-V nitrides are not currently available, measurements have been obtained from epitaxial films. Recent measurements of AlN thin films grown on SiC indicates a NEA [7] while a positve χ of 3.3 eV is measured for GaN on SiC.[8] The results for these and several alloy films are summarized in Fig. 1. The alloy concentration was deduced from cathodoluminescence measurements of the bandgap and the assumption of a linear relation between 3.4 eV for GaN and 6.2 eV for AlN. The results suggest that a negative electron affinity

is obtained for these surfaces with AlN percentages of ~70% or greater. To date there have not been measurements of the effect of surface adsorbates, but a theoretical analysis indicates that molecular adsorbates such as hydrogen will behave differently on the different nitride surfaces.[9]

Field Emission - Moving Probe

Field emission properties were measured using a position variable anode system. This technique has the advantage that the dependence of the emission on the anode to cathode spacing can be measured. In addition, the technique is not as sensitive to parallelism of the anode and cathode surfaces which often presents problems when using a spacer apparatus to measure field emission properties. Also, obtaining the high vacuum required for electron emission is accomplished more easily with the position dependent anode system, and the system is not susceptible to breakdown of the dielectric spacer.

Field emission measurements were applied to the p-type natural diamonds after various surface treatments.[6] Type IIb diamond (100) and (110) samples were prepared with the electrochemical cleaning processes and then loaded into the UHV moving probe field emission system. A (110) sample was also exposed to a hydrogen plasma and transferred directly to the field emission system. Field emission measurements were obtained at several distances, and the distance was determined by relating the measurements to the point of contact. This process leads to some uncertainty, but for these conducting substrates, it is not a critical issue. The average threshold field for the measurements is shown in Table 1. Here, very high values were obtained from the oxygen terminated surfaces and a low value was obtained from the hydrogen terminated surface.

While n-type diamond is not commonly available, single substitutional nitrogen doped

diamond can be prepared with a deep donor 1.7 eV below the conduction band. Geis et al. [10] have suggested that a Schottky contact, which is formed when type Ib single crystal diamond is metallized with nickel, may be sufficient to supply electrons into the conduction band of the diamond. In this model, the applied voltage would be dropped primarily across the metal/diamond interface, and a low field at the NEA surface would result in emission into vacuum. Figure 2 shows the field emission properties of a nitrogen doped diamond film grown on Si using [N]/[C] = 0.2. The average threshold field (for 10 nA emission) for this sample was 71 V/μm. After field emission measurements, damage to the diamond film and substrate was observed by optical microscopy. Micro-arcs between the sample and the anode are the most likely explanation for the observed damage. [11] These position dependent field emission measurements indicate that an injecting contact is not formed for these films. It is likely that the observed emission is directly from the Si substrate at the points of damage.

Field emission measurements have also been obtained from pyramid structures of Si doped GaN.[3] These structures are prepared by selective OMCVD growth processes.[3] We note that the surfaces were prepared with a hydrogen plasma exposure prior to the field emission measurements. This process was employed as an in situ cleaning process, and Auger electron spectroscopy verified removal of surface carbon contamination, but the treatment did not affect the monolayer surface oxide termination. The field emission results are presented in Fig. 3. This surface exhibits the lowest threshold of any sample that we have measured to date. Similar measurements from flat surfaces of similar films exhibit an average threshold field of ~50 V/μm.

PEEM Imaging of III-V-Nitride and Diamond Films

The technique of PEEM and FEEM has previously been applied to the study of CVD diamond thin films. Wang et al. [12] have reported electron emission from CVD diamond films with field strengths as low as 3V/μm, and it was suggested that the emission is due to the negative electron affinity of the diamond surfaces. In another study, Shovlin and Kordesch [13] report inducing low field cold emission in a partially oriented ([100] texture) diamond film by depositing 7nm of gold on the surface. While most studies have employed a Hg lamp to excite the PEEM image, synchrotron PEEM was performed on diamond films and uniform emission was observed. [14] We report in Figure 4 PEEM images comparing boron and nitrogen doped films. The images show emission from all surfaces with stronger emission from the edges near the surface. The differences in the images reflects the differences in the surface morphology as evidenced by SEM of the same samples. Raman analysis of these films shows a low concentration of sp^2 bonded carbon, and we do not detect enhanced emission from graphitic grain boundaries. The observed enhanced emission from the edges is likely due to field enhancement from the applied field of the microscope. For these samples we were not able to detect FEEM images. This is consistent with our field emission measurements which showed threshold emission fields greater than the 10V/μm available in the microscope system.

The PEEM and FEEM images of the Si doped GaN pyramidal array are displayed in Fig. 5. Note that emission is observed from the regions near the peaks of the GaN pyramids, and that emission intensity is nearly uniform for each of the emitters over the array. Moreover, emission is observed in the FEEM image, and this is again consistent with our field emission measurements which showed an emission threshold less than 10 V/μm.

Concluding Remarks

The results presented here demonstrate the necessaity for a series of complimentary measurements in order to characterize the properties of wide bandgap materials for electron emission applications. It is evident that the electron affinity is a critical limiting aspect for field emission from conducting p-type diamond and Si doped GaN. It appears that the electron emission from p-type diamond is from the valence band of the material, while evidence suggests that the field emission from Si-doped GaN originates from electrons in the conduction band. Moreover, we were not able to obtain emission from nitrogen doped diamond without damaging the surfaces. This suggests that the emission threshold is greater than the measured value of ~70V/μm. The high field required for emission from these samples seems inconsistent with the proposed model for the effect of single substitutional nitrogen. The PEEM measurements were fully consistent with the field emission measurements. In the PEEM from diamond, emission was observed from all surfaces with some enhancement at the edges. This was attributed to the field in the microscope.

The Si doped GaN pyramid structures displayed the lowest field emission threshold of our samples, and both PEEM and FEEM emission showed relatively uniform emission originating from the peaks of the structures.

Another technique that is critical for characterizing field emission materials is field emission energy distribution (FEED). In this technique the energy spectrum of the emitted electrons is analyzed. This technique is important because the energy of the emitted electrons can be determined with respect to the contact Fermi level. This allows determination of whether

the emission is from metallic states at the Fermi level or from the valence or conduction bands of a semiconductor.

The results for the diamond-type material systems described here show promise for the development of cold cathode emitters. While relatively low field emission thresholds have been reported for p-type diamond, the development of n-type doping could certainly improve the performance of diamond based emitters. For the nitrides, it appears that n-type GaN holds real promise as an electron emitter. The development of selective growth processes to produce pyramid structures which combine the low work function and field enhancement is one approach. Another will be to explore AlGaN alloys with increased Al concentration while still maintaining n-type doping. To date n-type character has been reported for AlGaN alloys with ~40% AlN, and theoretical analysis suggests that doping of alloys with up to 60% AlN is possible. There have been no reports to date on the effects of different surface terminations of the nitrides, while it is now established that surface termination strongly affects the emission character of diamond surfaces. Future research is in progress to address these issues.

Acknowledgments: We gratefully acknowledge Harald Ade for discussions on the PEEM measurements, and we are very appreciative of O.K. Nam and R.F. Davis for supplying the nitride samples employed here and in our previous studies. We also acknowledge the Duke University FEL Laboratory for access to the OK-4 UV FEL. This project was supported through the Office of Naval Research.

REFERENCES

1. F.J. Himpsel, J.A. Knapp, J.A. van Vechten, D.E. Eastman, Phys. Rev. B 20, 624 (1979).
2. B.B. Pate, Surf. Sci. 165, 83 (1986).
3. O.-H. Nam, M.D. Bremser, B.L. Ward, R.J. Nemanich, and R.F. Davis, Jpn. J. Appl. Phys. 36, L532 (1997).
4. J. van der Weide and R.J. Nemanich, Phys. Rev. B, **49** (1994) 13629.
5. C. Bandis, and B.B. Pate, Phys. Rev. Lett. 74, 777 (1995).
6. P.K. Baumann and R.J. Nemanich, Surface Science, (in press).
7. M. C. Benjamin, C. Wang, R. F. Davis, and R. J. Nemanich, Appl. Phys. Lett. **64**, 3288 (1994).
8. M.C. Benjamin, M.D. Bremser, T.W. Weeks, Jr., S.W. King, R.F. Davis, and R.J. Nemanich. Applied Surface Science 104/105, 455 (1996)
9. R.J. Nemanich, M.C. Benjamin, S.W. King, M.D. Bremser, R.F. Davis, B. Chen, Z. Zhang, and J. Bernholc. *Gallium Nitride and Related Materials*, edited by F.A. Ponce, R.D. Dupuis, S. Nakamura and J.A. Edmond. (Mater. Res. Soc. Symp. Proc. vol **395,** 1995) pp 777-788.
10. M.W. Geis, J.C. Twichell, J. Macaulay, and K. Okano, Appl. Phys. Lett. 67, 1328 (1995).
11. O.M. Kuttel, O Groning, E. Schaller, L. Diedrich, P. Groning and L. Schlapbach, Diamond and Related Mater. 5, 807 (1996).
12. C. Wang A. Garcia D.C. Ingram M. Lake, M.E. Kordesch, Electronic Lett. 27, 1459 (199?)
13. J.D. Shovlin, M.E. Kordesch, Appl. Phys. Letters 65, 863 (1994)
14. J.D. Shovlin, M.E. Kordesch, D. Dunham, B.P. Toner, W. Engel, J. Vac. Sci. Technol. A 13, 1111 (1995).

Table 1. Summary of the UPS results on (100), (111) and (110) type IIb natural diamond surfaces. (RT: room temperature, χ: electron affinity, PEA: positive electron affinity, NEA: negative electron affinity) Unless noted otherwise the surfaces have been cleaned by an electrochemical etch. The experimental uncertainties are 0.1 eV. Also field emission results of C(100) and (110) and are shown.

Surface	Sequence of Annealing or H-plasma Treatment			
	500°C	900°C	1100°C	
C(100) after chromic acid clean	PEA, χ = 1.00 eV	PEA, χ = 0.70 eV	NEA, χ < 0	
C(100) after electrochemical etch	PEA, χ = 1.45 eV	NEA, χ < 0	PEA, = 0.75 eV	
	900°C	H-plasma	1100°C	H-plasma
C(100) after electrochemical etch	NEA, χ < 0	NEA, χ < 0	PEA, = 0.75 eV	NEA, χ < 0
	RT to 600°C	H-plasma	900°C	
C(111) after chromic acid clean or electrochemical etch	NEA, χ < 0	NEA, χ < 0	PEA, χ = 0.5 eV	
	700°C	800°C	H plasma	800°C
C(110) after electrochemical etch	NEA, χ < 0	PEA, χ = 0.6 eV	NEA, χ < 0	PEA, χ = 0.6 eV

	Field Emission threshold
C(100) after electrochemical etch	79 V/μm
C(110) after electrochemical etch	81 V/μm
C(110) after H plasma treatment	25 V/μm

Figure Captions

1. Plot of the electron affinity versus alloy concentration for AlGaN alloy films grown on 6H-SiC (0001). The values were deduced from UV photoemission, and we note that negative values cannot be obtained with this technique.

2. Field emission measurements of a nitrogen doped diamond film obtained at various anode to sample distances (a), and an analysis of the average field required to obtain an emission current of 10 nA (b). In (a) the current has been normalized by the background noise current and is plotted on a log scale (I_{noise} = 0.1 nA). The distance scale in (b) was measured relative to the first measurement position, and subsequent data were obtained as the anode was moved towards the surface. The slope of the plot in (b) is 71 V/μm.

3. Field emission measurements of a Si doped GaN pyramid array. The measurements were obtained at various anode to sample distances (a), and an analysis of the average field required to obtain an emission current of 10 nA (b). The slope of the plot in (b) is 7 V/μm.

4. PEEM image of p-type diamond film (a) and a nitrogen doped film (b). In these images the dark regions represent the areas of intense electron emission. A 100W Hg lamp was used to obtain (a) while the spontaneous radiation from the UV FEL at Duke University was used to obtain (b).

5. PEEM image of the pyramid structures of the Si doped GaN (a), and FEEM image of the same surface (b). In these images the dark regions represent the areas of intense electron emission. The images were excited with a 100 W Hg lamp.

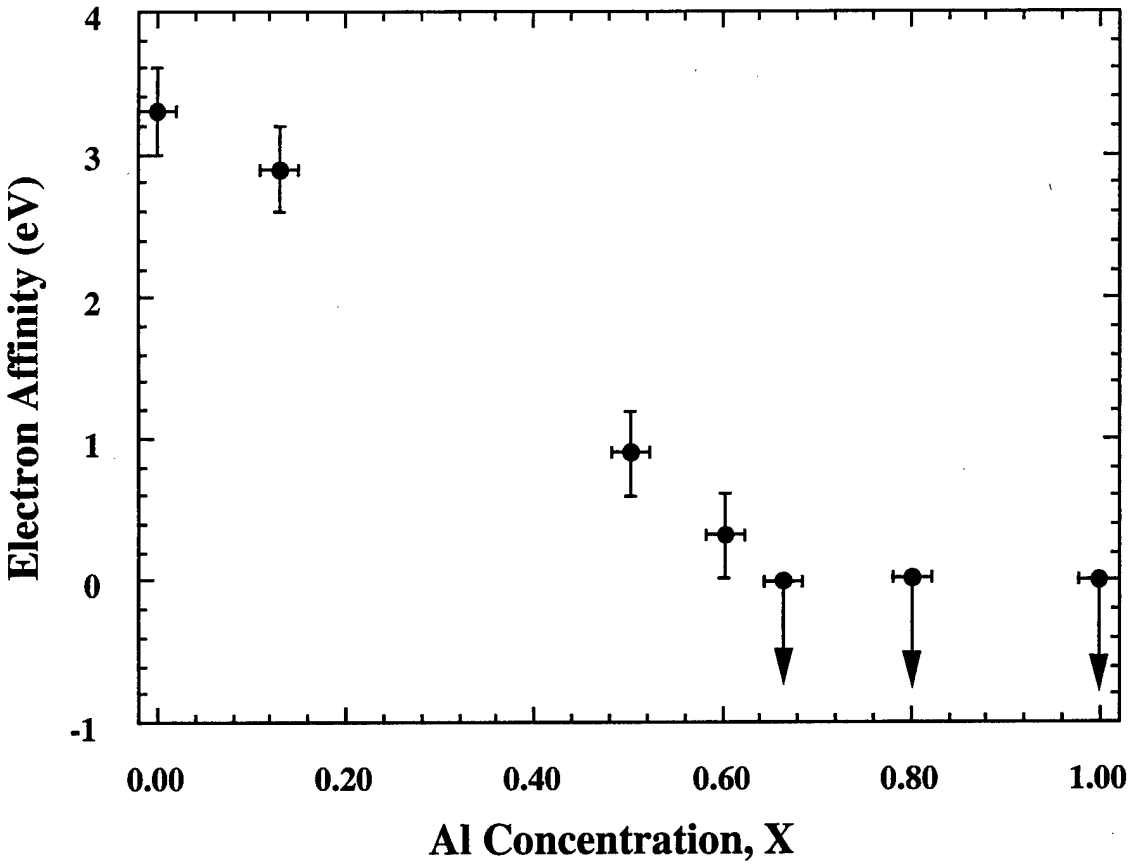
Electron Affinity (eV)
4
3
2
1
0
-1
0.00
0.20
0.40
0.60
0.80
1.00
Al Concentration, X

Figure 1

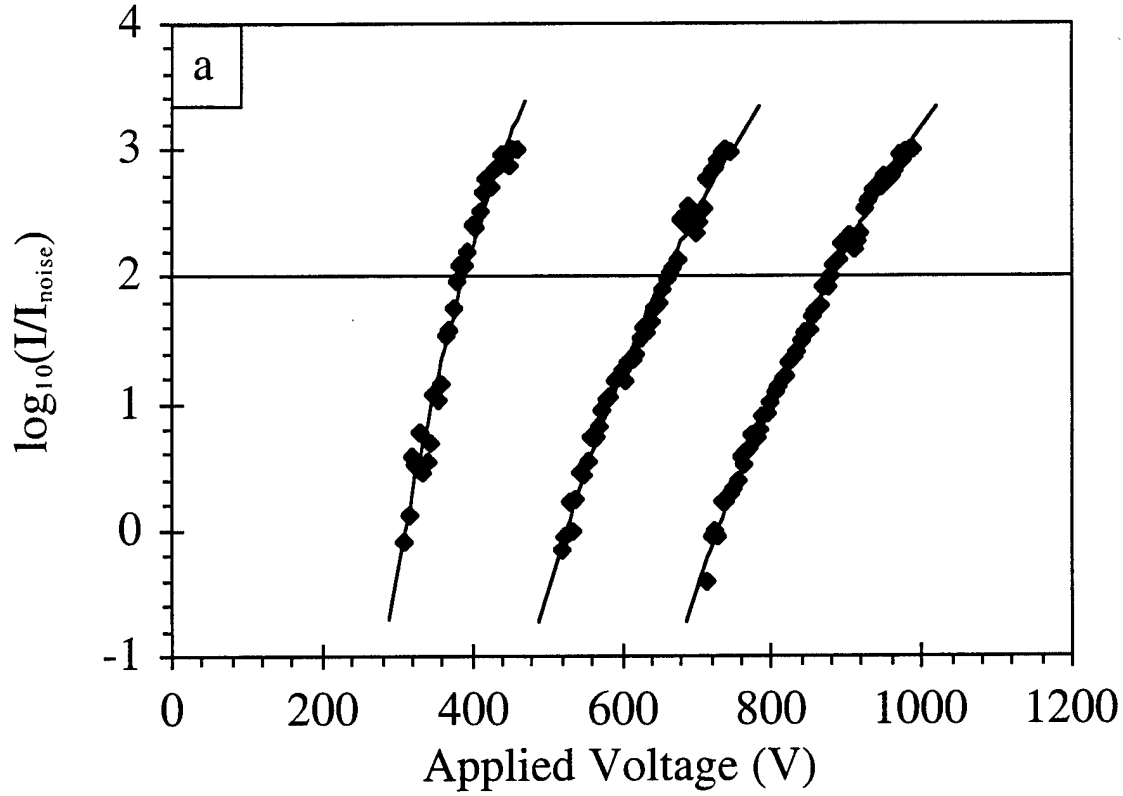
a
4
3
2
1
0
-1
$\log_{10}(I/I_{noise})$
0
200
400
600
800
1000
1200
Applied Voltage (V)

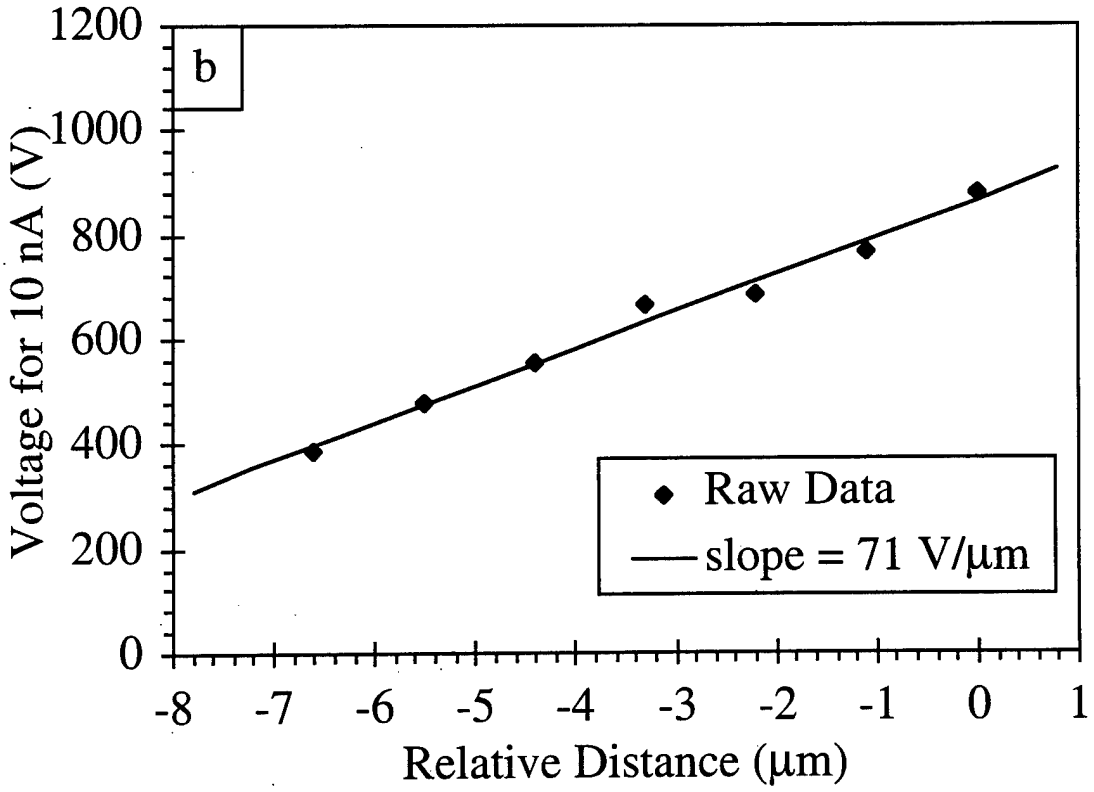
b
1200
1000
800
600
400
200
0
Voltage for 10 nA (V)
Raw Data
slope = 71 V/μm
-8
-7
-6
-5
-4
-3
-2
-1
0
1
Relative Distance (μm)

Figure 2

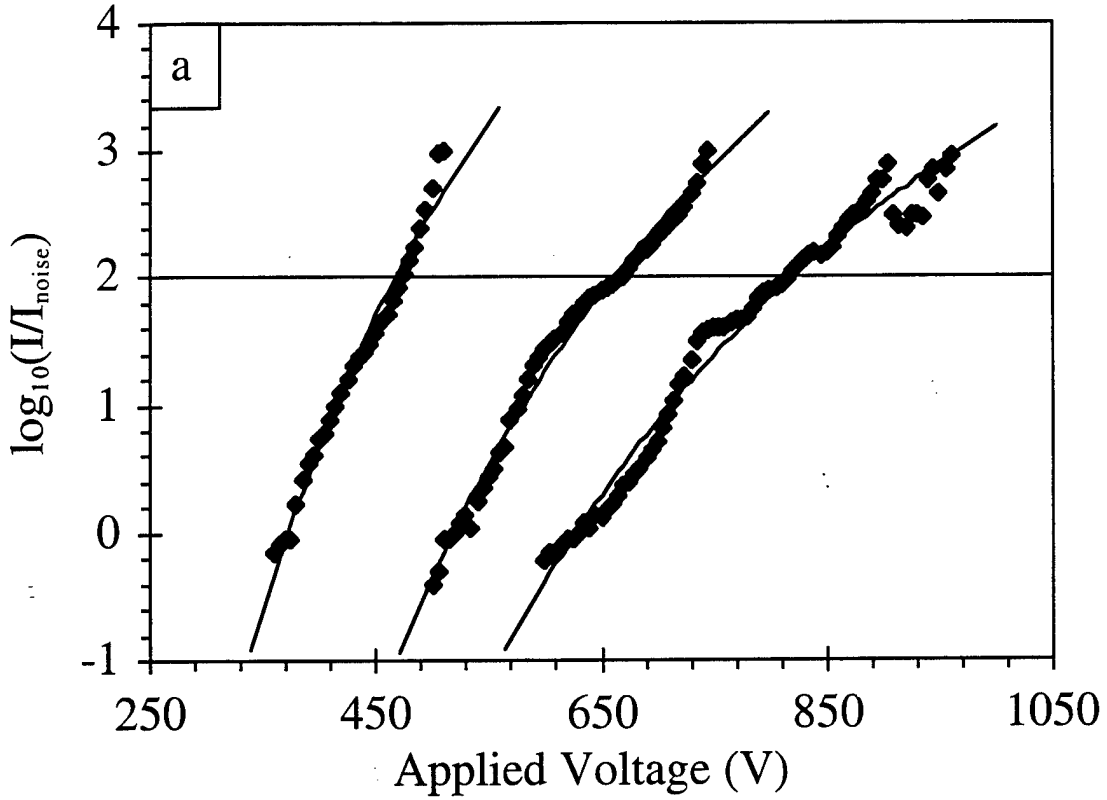
a
4
3
2
1
0
-1
$\log_{10}(I/I_{noise})$
250
450
650
850
1050
Applied Voltage (V)

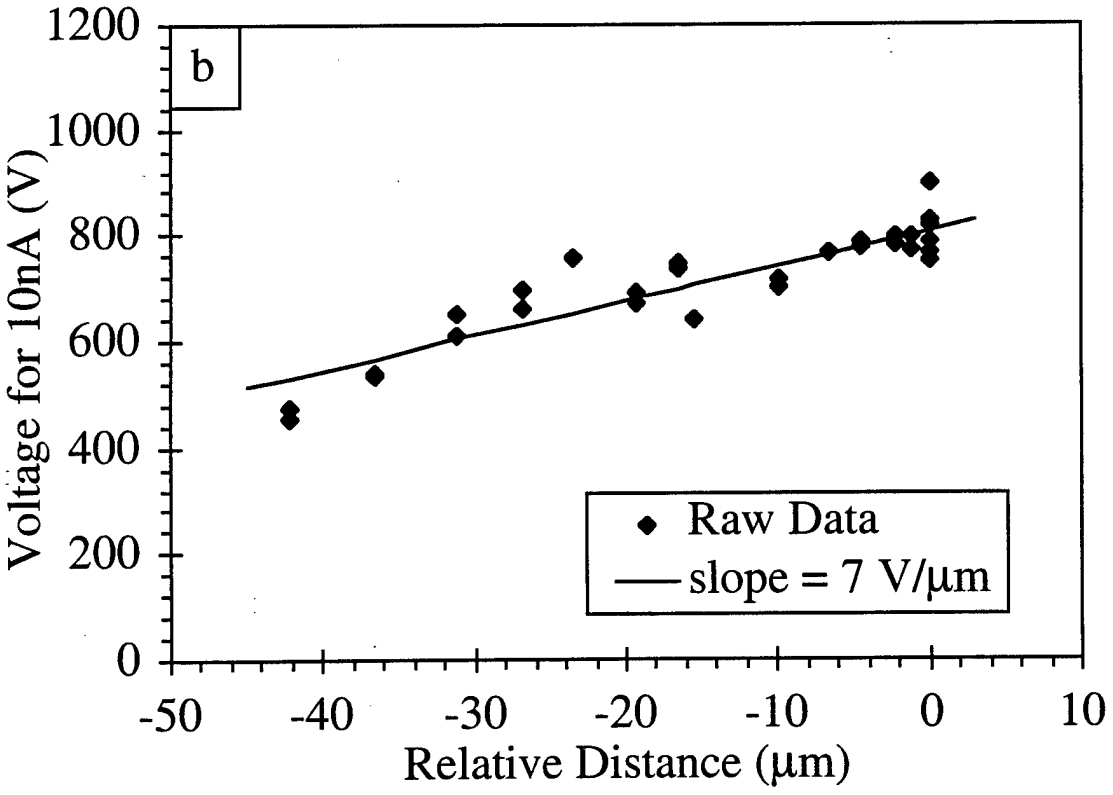
b
1200
1000
800
600
400
200
0
Voltage for 10nA (V)
-50
-40
-30
-20
-10
0
10
Relative Distance (μm)
Raw Data
slope = 7 V/μm

Figure 3

a)

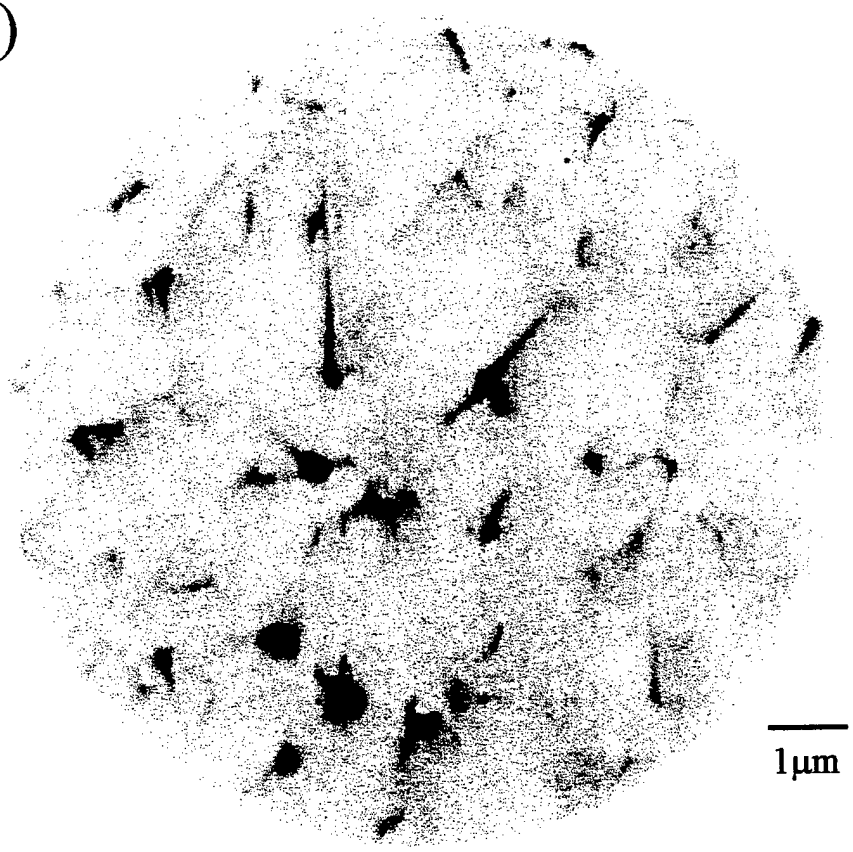

Figure 4a

b)

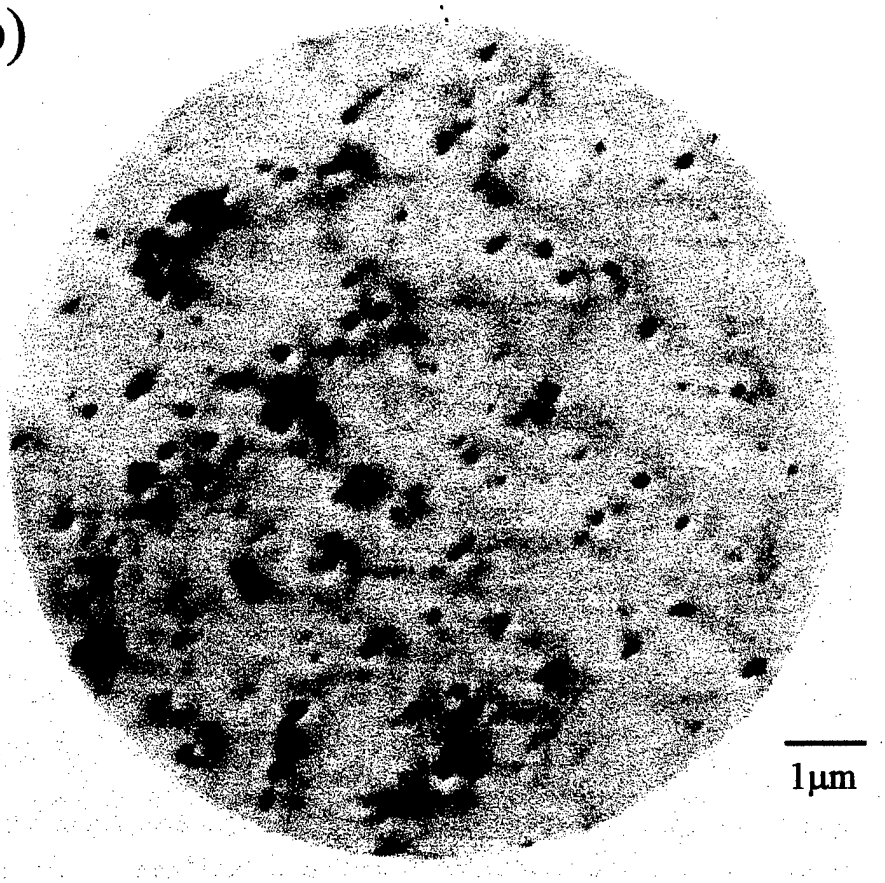

Figure 4b

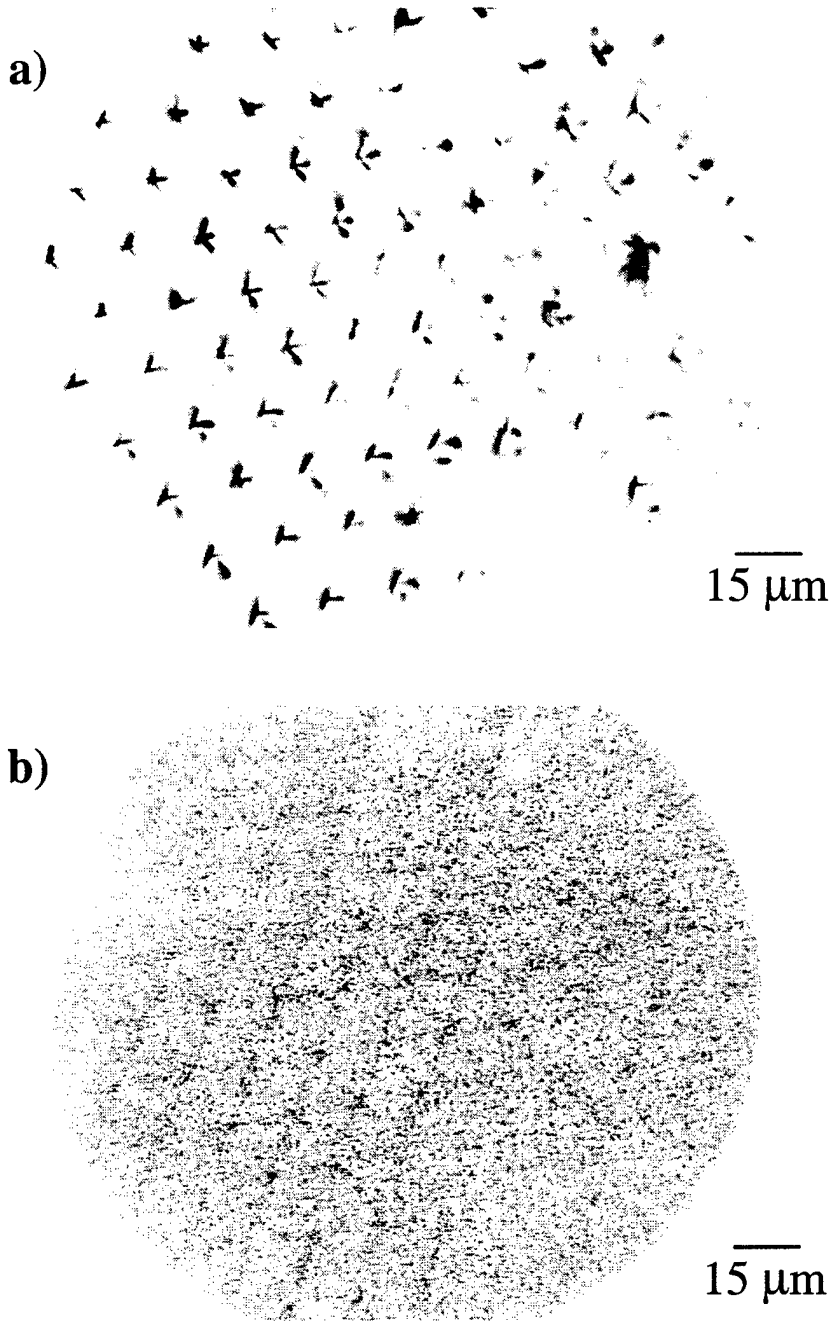

Figure 5

Photoemission Electron Microscopy of buried Ti/AlN Interfaces

J. Hartman, S. English, W. Yang, H. Ade, R. Nemanich, R. Davis

A. Abstract.

The use of a Photo-Emission Electron Microscope for the investigation of buried Ti contacts was investigated. The contacts consisted 100 μm Ti circular dots that were buried under 400 Å AlN and were deposited on a SiC substrate and a GaN epilayer. Results show that upon heating to 300 – 400 °C the contrast mechanism between the buried contacts and the background disappears when viewed with the mercury arc lamp. Upon repeating the PEEM experiment after the sample has been at atmosphere for several days, the contrast mechanism returns. The PEEM, with use of the Free Electron Laser at Duke University, also showed the underlying structure of the surface, which was not visible with the mercury arc lamp.

B. Introduction

The use of wideband semi-conducting materials has gained widespread interest due to their potential applications as light emitting diodes and field effect transistors [1]. Recent advancements have produced blue LED's from metalorganic chemical vapor deposition [2] and laser diodes [3] in both the United States and abroad. These devices have been primarily made from MOCVD grown material, since it produces the best quality [3]. However, molecular beam epitaxy is a powerful tool due its ability to control growth on a monolayer level [3]. This report presents our most recent advancements concerning the set-up and use of the Photoemission Electron Microscope

(PEEM) and molecular beam epitaxy chamber (MBE) to characterize AlN and GaN. Results from an experiment of buried Ti interfaces (contacts) are presented below.

Over the past several years, continuing development of the resolution of Photoemission electron microscopes has allowed the microscopic analysis of surfaces and interfaces. Recent studies have used the PEEM for the analysis of p-n junctions [4], buried interfaces [5], Schottky contacts [6], electromigration [7], and adsorption (desorption) [7]. In PEEM, the sample is illuminated with a light source. Photons with an energy greater than the work function result in emission of an electron. Photoemitted electrons are then accelerated in a 20 kV field. The electrons are imaged using a multichannel plate and phosphor screen. The image contrast is due to differences in the photoyield of the electrons emitted which occurs due to differences in topography or differences in work function.

Using PEEM we have examined buried 100 μm Ti contacts under an 400 Å of CVD AlN. The measurement of the buried Ti dots show a potential method for the characterization of buried interfaces and possibly characterizing band bending at these interfaces [6]. The chemical reactions associated with the interface may also be characterized through analysis of the difference in work functions associated with areas of different chemical composition [5].

C. Equipment Accomplishments to Date

Over the past several months, our group has had the opportunity assemble a custom built Molecular Beam Epitaxy chamber with an attached Auger system. This system will allow the growth and characterization of III-N epitaxy semiconductor films, but still allow monolayer control. The system consists of two EPI knudsen cells; one for Al and one for Ga. The nitrogen source at this time is an RF plasma source from SVT Associates, however, we plan to employ ammonia as the source in the near future. The system is pumped using two ion pumps obtained from Physical Electronics. These consist of an 80 l/s for the Auger system and 520 l/s for the MBE system. During nitride growth, the gate values to the ion pumps will be closed and pumping will be done using a 520 l/s turbo-molecular drag pump from Pfeiffer. The first AlN film was grown on June 16th, 1998. However, due to the new system with new sources, this film had high levels of oxygen. Over the next few months, the system will be optimized for nitride growth.

As stated above, along with the Molecular Beam Epitaxy system, a Physical Electronics Auger system was also assembled. The system consists of a 10-155 cylindrical mirror analyzer and can supply an electron beam voltage up to 5kV. The Auger system is attached directly to the MBE chamber for characterization of the films and substrates before and after a growth run.

In the very near future, a linear 4-pocket e-gun from Thermionics will be added to the chamber. This will allow cleaning of SiC films and deposition of metals for various contacts to the semiconductors.

D. Experimental Procedures: Buried interfaces

The sample preparation for buried Ti contact experiments consisted of evaporating 250 Å of Ti on an epilayer of GaN grown on a (0001) 6H SiC substrate using a custom MBE chamber and on a 6H-SiC substrate by through the use of a Themionics 5 pocket linear e-Gun (Model 100-0050). The pattern consisted of 100 μm dots, created using a standard Molybdenum screen. A capping layer of 400 Å of AlN was then grown over the Ti dots using CVD. The samples were loaded into a commercial Photoemission Electron Microscope manufactured by Elimitec. Analysis was conducted using light from a ORIEL mercury arc lamp and spontaneous emission spectrum from 3.9 eV to 6.3 eV created by Duke University's Free Electron Laser (FEL). The FEL allowed observation of the Ti contacts at specific photon energies. The samples were viewed at temperatures between 300K and 983 K.

E. Results: Buried interfaces.

The first sample tested consisted of the Ti dots deposited on SiC. During the first run, in which only the mercury arc lamp was used, the Ti contacts appeared to have disappeared upon heating to 425 °C (Figures 1 and 2). Upon cooling the contacts became visible again, but had the same contrast as the background. However, after several days at atmosphere, upon analyzing the samples for a second time with the mercury arc lamp, the contacts had reappeared and upon heating disappeared for a second time. The sample was then run using spontaneous emission of light from Duke's FEL. This time the Ti

dots did not disappear at 425 °C, even at the 5.1 eV characteristic energy of the Mercury arc lamp (Figure 3 and 4).

Another phenomena that was noticed when observations were made with the FEL was the visibility of the many details of the surface and/or underlying structures. At this point it is not clear as to whether these structures are on the surface or a result of the finish of the polishing of SiC wafer underneath the AlN layer. Surface characterization using SEM and TEM will be conducted in the near future.

The results from the analysis of the Ti contact on the GaN sample were different in some aspects. The contacts had appeared to disappear upon heating to 286 °C using the mercury arc lamp and at 700 ° C using the FEL (Figures 5-8). However, the pictures contained much more noise than those of the Ti contacts on the SiC. This limited the visibility of the underlying surface of the GaN. This background noise may be due to the lower bandgap associated with GaN under the AlN or due to the morphology of the AlN grown on GaN.

F: Discussion

This project was conducted to determine the possibility of using the Photoemission Electron Microscopy for the observation of buried interfaces. The band diagram associated with such a metal/semiconductor interface is shown in Figure 9. The electrons are excited above the band gap of the AlN, and due to the potential field accelerated away from the sample. Further analysis of the interface should produce a more detailed band structure once the interface compounds have been identified.

The Ti contacts on the SiC have produced the most varied results. Initial experiments had shown, that these contacts produced a sharper image than those of the Ti contacts on the GaN. This may be due to n-type doping of the GaN, which would allow more electrons to be excited into the conduction band and through the AlN. A second possibility is that the Ti contacts have produced Ti/Ga/N compounds and Ti silicides. The morphology of AlN on the GaN may have also contributed to the increased noise levels.

The disappearance of the dots in both cases, may be attributed to defect states within the AlN epilayer. This would allow the electrons to tunnel through the AlN with the photon energies at which these samples were analyzed. This theory is supported by the fact that we can heat the sample and make the contacts disappear, and after a few days at atmosphere, upon repeating the PEEM measurements, the contacts are again observable. Also, there may be effects due to the absorption of hydrogen, water, and oxygen. A previous study[4] has shown that the contrast differences before and after heating may be affected by the surface states. This same process may be evident in the disappearance of the Ti dots.

G: Conclusion

Photo-Emission Electron Microscopy has been used to view buried contacts under a wideband gap semiconductor. The Ti contacts on both substrates disappear upon heating to 300 – 400 °C when imaging with the mercury arc lamp. Future research will

explore the possible origins of the loss of contrast. More importantly, the results presented here demonstrate that PEEM can be applied to examine buried interfaces.

H: Reference:

[1] E.J. Tarsa, B. Heying, X.H. Wu, P. Fini, S.P. DenBaars, and J.S. Speck, J. Applied Phys., **82**(11), 5472 (1997).

[2] Akihiko Kikuchi, Hiroyuki Hoshi, and Katsumi, Jpn. J. Appl. Phys., **34**, Part 1, No 2B, 1153 (1995).

[3] N. Gradjean, J. Massies, P. Vennegues, M. Leroux, F. Demangeot, M. Renucci, and J. Frandon., J. Appl. Phys., **83** (3), 1379 (1998).

[4] M. Giesen, R.J. Phaneuf, E.D. Williams, T.L. Einstein, and H. Ibach., Appl. Phys. A, **64**, 423 (1997).

[5] J. Almeida, C. Coluzza, T. dell'Orto, F. Barbo, M. Bertolo, A. Bianco, S. Cerasari, S. Fontana, and G. Margaritondo., J. Appl. Phys. **80** (3), 1460 (1996).

[6] Margret Giesen, Raymond J. Phaneuf, Ellen D. Williams, and Theordore L. Einstein., Surface Science, **396**, 411 (1998).

[7] Y. Shidahara, K. Aoki, Y. Tanishiro, H. Minoda, and K. Yagi., Surface Science, **357-358**, 820 (1996).

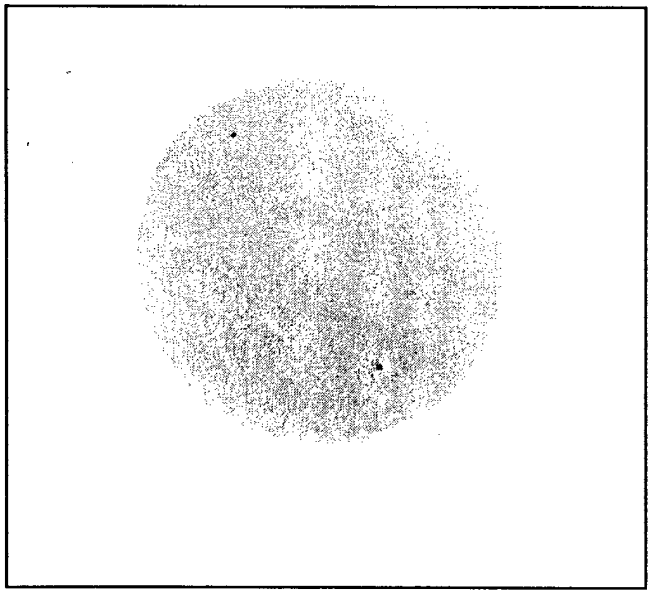

Figure 1: Buried 100 μm Ti contact under 400 Å of AlN on SiC. Image was taken at Room Temperature with the mercury arc lamp.

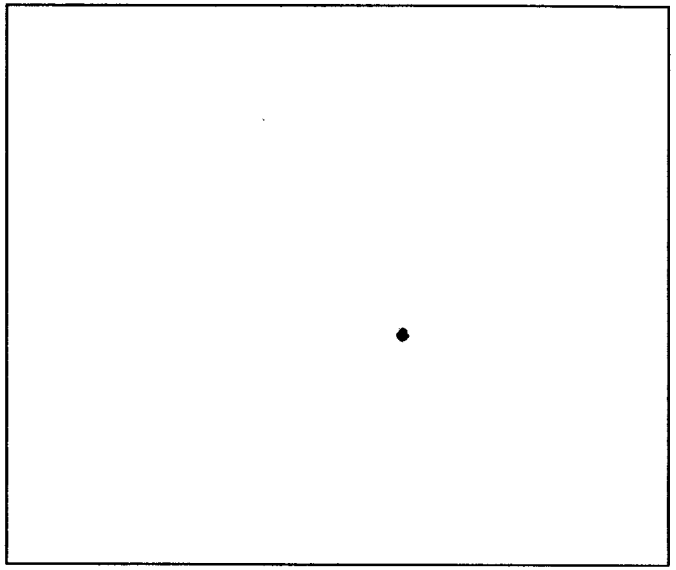

Figure 2: Same Ti contact as Figure 1. This image is taken at a temperature of 425° C

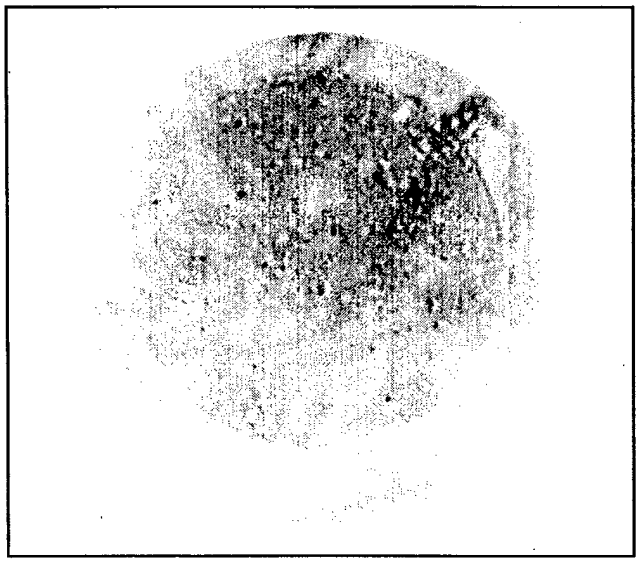

Figure 3: Buried 100 μm Ti contact under 400 Å of AlN on SiC substrate imaged with the Duke University's Free Electron Laser (FEL) at 5.5 eV. Image was taken at Room Temperature

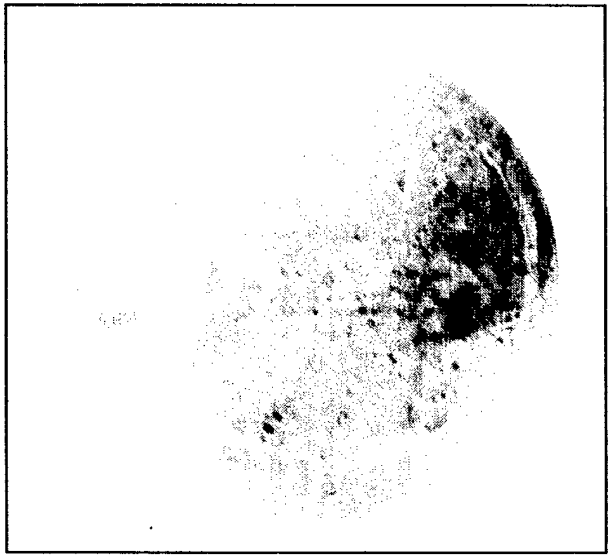

Figure 4: Same buried contact as Figure 3. Image was taken at a temperature of 525° C.

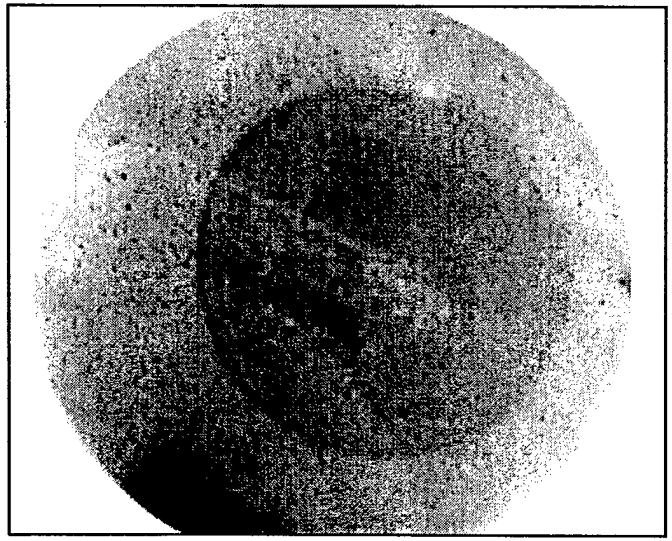

Figure 5: Buried 100 μm Ti contact under 400 Å of AlN on GaN epilayer. Image was taken at Room Temperature with the mercury arc lamp.

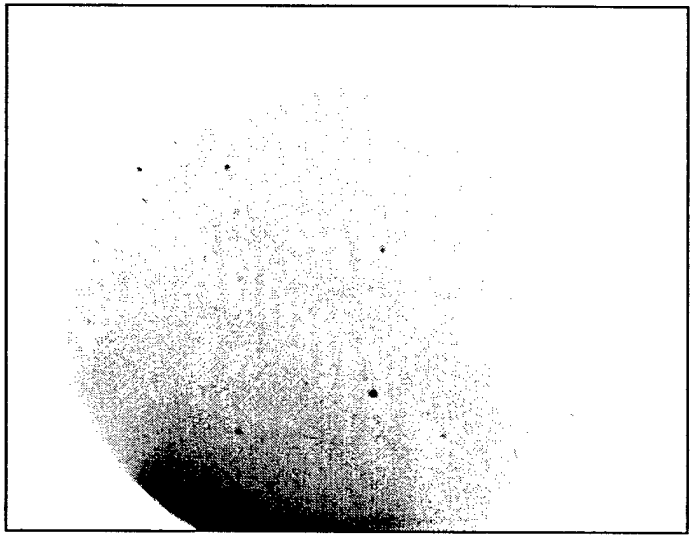

Figure 6: Same buried Ti contact as Figure 5. This image was taken at a temperature of 286 °C. The contact was held at temperature for 11 minutes.

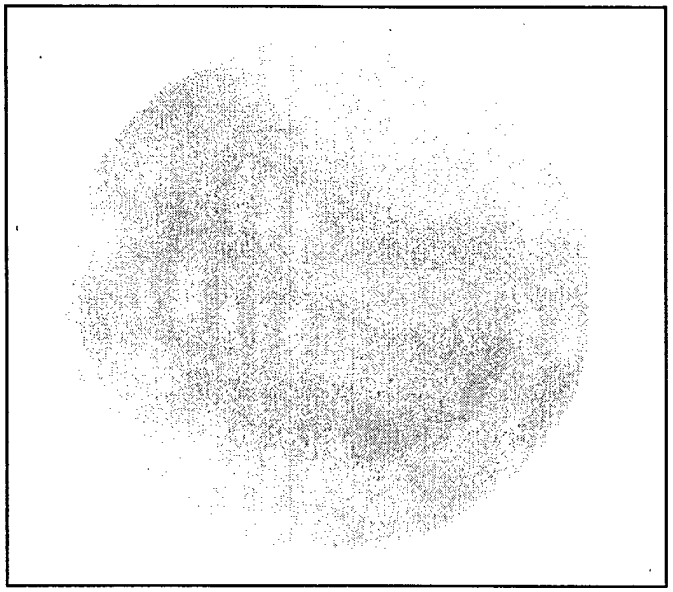

Figure 7: Buried 100 μm Ti contact under 400 Å of AlN on GaN epilayer imaged with the Duke University's Free Electron Laser (FEL) at 5.4 eV. Image was taken at Room Temperature Room Temperature

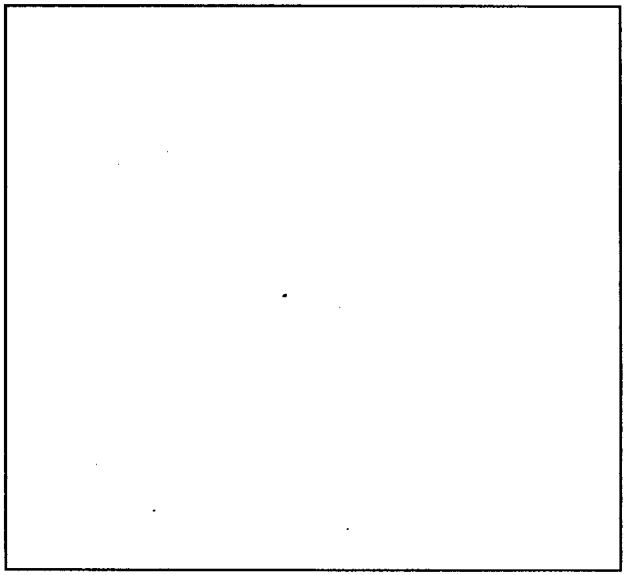

Figure 8: Same buried contact as Figure 7. Image taken with the Duke University's Free Electron Laser (FEL) at 5.5 eV at 700 °C.

Band Diagram for the Ti/AlN Interface under a Bias Voltage

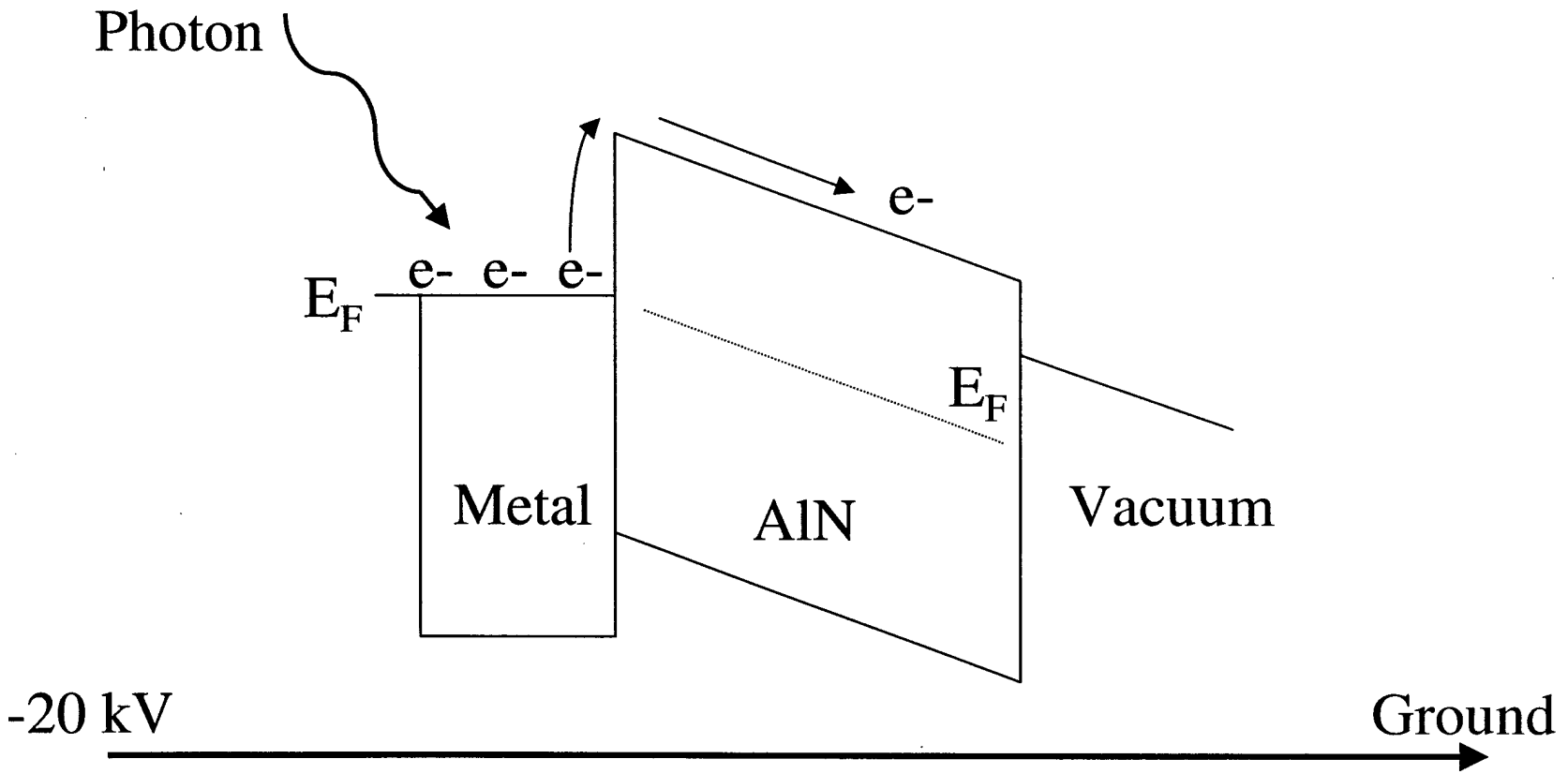

Figure 9: Possible band structure of buried Ti contact under a bias voltage

REAL-TIME OBSERVATION OF TI SILICIDE EPITAXIAL ISLANDS GROWTH WITH THE PHOTOELECTRON EMISSION MICROSCOPY

W. Yang, H. Ade and R.J. Nemanich,

Department of Physics, North Carolina State University, Raleigh, NC 27695- 8202

ABSTRACT

The formation of nanoscale Ti silicide islands was observed by Photo-electron emission microscopy (PEEM). The islands were prepared by deposition of an ultrathin Ti (3-12ML) on Si(001) at room temperature and at an elevated temperature of 950°C. The island formation was initiated by *in situ* annealing to 1150°C. It was observed that initially Ti silicide islands form while longer annealing indicates some islands move and coalesce with other islands. Most of the islands are similar in size and have relatively uniform separation. Also, it was shown that for continued Ti deposition at a temperature of 950°C, the density of islands did not increase. However, islands grew together when their perimeter lines touch each other. The results are described in terms of island growth processes of coalescence and ripening.

INTRODUCTION

Photo-electron emission microscopy (PEEM) is an emission microscopy technique in which images of a solid surface are formed by photo excited electrons. Typically, ultra violet (UV) light above the photoelectron threshold will cause electrons to be emitted from a surface. The photo excited electrons originate from the near surface region (~10nm), and essentially reflect the electronic structure of the surface. These electrons may be accelerated and imaged, and the image will reflect the properties of the surface. PEEM has already been used to investigate surface chemistry of metals [1], epitaxial growth of materials [2] and characterization of semiconductor devices [3]. PEEM allows real time observation and direct imaging during processing with monolayer surface sensitivity and high resolution (~10nm). For this reason, PEEM is particularly suited for measurement of dynamical processes on semiconductor surfaces.

In this study, PEEM is used to obtain the growth of nanoscale epitaxial silicide islands on Si surface. The image contrast mechanism for a metal on a semiconductor system is the energy difference between the work function (WF) of a metal and the photo-threshold of the semiconductor (The semiconductor photo-threshold is the energy to excite an electron from the valence band to the vacuum level). Therefore, $TiSi_2$ islands on a Si surface would be imaged by this contrast mechanism. The photon energy of the employed UV-light should be below the photo-threshold of silicon and above the WF of the Ti silicide. In this case, electrons will be emitted from regions with Ti and no emission will occur from exposed Si surfaces.

Our previous studies have shown the tendency of $TiSi_2$ on Si to form epitaxial island structures. Furthermore, for ultrathin Ti (<1nm) deposited on Si substrate followed by high temperature annealing (~1000°C), similarly sized islands of Ti silicide (~30nm) were obtained to be uniformly distributed over the Si (001) surface [4-6]. The Ti silicide island size and spatial distribution were very dependent on the growth conditions (i.e. Ti layer thickness, annealing temperature and surface roughness)[4,5]. It was suggested that the narrow island distribution is due to surface diffusion and the strain field effect induced in the substrate by the islands.

In this study, the formation of Ti silicide islands is explored with thin Ti deposition of 3-12 monolayers(ML) on Si(001) substrates. During in situ annealing at temperatures up to 1150°C, the island formation process and dynamics are observed in real-time with PEEM. After Ti silicide island formation, the surfaces are *ex-situ* analyzed with AFM and SEM to compare the surface morphology with the results from the PEEM. The size and distribution of islands are obtained, and the island growth is explained in terms of coalescence and ripening growth processes.

EXPERIMENT

The experiments were performed in an UHV PEEM system obtained from Elmitech. This system allowed heating of the substrates to > 1200°C, and the chamber is equipped with a Ti-filament deposition source. The base pressure in this system was $< 2 \times 10^{-10}$ Torr. The electric potential used for accelerating the imaging electrons is approximately 20kV across a gap of

2mm. The UV-light source is a Hg discharge lamp with upper cut-off energy near 5.1eV. We have demonstrated the resolution of our system to be ~12nm using a 100W Hg lamp as the UV excitation.

Sections of silicon (001) wafers (n-type, P-doped, resistivity 0.8-1.2 Ω-cm, 9x9mm^2) were used as substrates. The wafers were cleaned first by uv-ozone exposure and then by an HF based spin etch (HF:H_2O:ethanal=1:1:10). After *ex-situ* cleaning, the wafers were mounted to the sample holder and then introduced into the PEEM chamber. Before Ti deposition, the wafer was heated at a temperature of 800°C for 10 minutes by filament radiation and electron bombardment from the backside in a sample holder. The residual oxide and hydrogen were removed by the heat treatment. After cleaning, RHEED displayed a 2x1 pattern typical of the Si(001) reconstructed surface. Titanium was deposited *in situ* from the hot-filament titanium source in the PEEM chamber onto the cleaned sample which was held at room temperature or a temperature of 950°C. The titanium layer thickness was 3-12 monolayers (ML) with a deposition rate of 1ML/20S. To observe the Ti silicide island formation process, the substrates were annealed in UHV from 100°C up to 1200°C in 100°C increments for intervals of 10 minutes.

The PEEM images were displayed with a microchannel plate and phosphor screen installed in the PEEM which was monitored with a CCD camera. The images were simultaneously stored digitally with an image processor and on video tape. Image acquisition was obtained with a real-time image processor (DSP-2000) which is capable of integration of up to 128 single frames. For the data presented here, sixteen successive images were integrated. The resulting images correspond to a signal integrated over 16/30th of a second. After the

substrates were unloaded from the PEEM, *ex-situ* AFM and SEM were performed to compare the surface morphology.

RESULTS

Initially, we monitored the surface morphology and the Ti silicide island formation processes while titanium is deposited on a clean Si(001) substrate followed by annealing to 1150°C. The PEEM images showed the overall surface of the Si as bright for the as-loaded wafers which became uniformly dark after the heat cleaning. The results suggest that the photo-threshold of the oxide terminated and the cleaned surfaces are below and above cut-off energy of Hg lamp(5.1eV), respectively. After Ti deposition of 10ML on the clean surface, the image is uniformly bright as the whole surface was covered uniformly by titanium (the WF of Ti is ~4.4eV). During annealing up to 700°C, the images of the surface did not change but grew darker. The darker surface indicates that the Si from the substrate has diffused into the overlayer of Ti, and a Ti silicide phase has formed. Our previous study showed Ti silicide island formation at this temperature [6]. One possibility to explain these inconsistent results may be that the photoelectron yield is too low to image the small islands. However, as shown in Fig. 1 separated

$TiSi_2$ islands were observed after annealing at 1000°C. The image contrast originates from the photo-threshold difference between $TiSi_2$ (~4.6eV) and Si (>5.1eV).

Fig. 1 shows a sequential PEEM image of the $TiSi_2$ island formation sequence as the substrate is held at 1150°C for 15 minutes. Initially, similar sized islands are distributed uniformly and completely separated (Fig. 1-a). As the annealing time increases, the average size of the islands increases gradually, and the number of islands decreases (Fig. 1-f). Fig. 2 shows that the number of islands decreases for longer annealing time. The data is fitted with an exponential. Examination of islands highlighted by the circles in Fig. 1(b)-(e) indicates a coalescence growth process. The islands, with substantial thermal energy, diffuse on the surface. In this sequence, close islands are observed to combine with each other and transform into larger islands. The triangles in Fig. 1(c)-(f) display another island growth process. The large islands grow larger while the small islands disappear. This is characteristic of ripening integrated by surface diffusion.

Ex-situ AFM measurements of the same sample also display a uniform lateral and vertical size of the islands (Fig. 3). The average lateral size of the islands is ~500nm and the height is ~200nm. In comparison with our previous study (diameter of island: 50nm, height: 5nm) [4], the islands are larger and are separated by greater distances. This difference is attributed to different growth conditions (increased Ti thickness and higher annealing temperature). The SEM measurements also show a similar island distribution. The shape of the islands could be observed by tilting the sample be 60°[Fig. 4]. The larger islands are observed to be flatter than smaller ones. An interesting aspect of the shape of islands is the bump of Si under each island [Fig. 4-a]. This shape may be influenced by the high electric field of $\sim 10^7$ V/m between the sample and cathode lens of the PEEM.

To monitor the island formation during deposition at an elevated temperature, 3-12ML of

Ti was deposited continuously at a temperature of 950°C (Fig. 5). It was observed that the growth mode of the Ti silicide at the high temperature is 3d-island growth (Volmer-Weber mode). Also, more dense and smaller islands were formed compared with Ti deposition followed by annealing at the same temperature. The density and average size of the islands did not increase even though the Ti thickness increased. However, islands next to each other coalesced as the deposition thickness of Ti increases. In order to observe the motion and coalescence of these islands, it would be necessary to obtain images with higher magnification. Unfortunately, the low intensity of the electron emission from these samples limited the magnification of the PEEM.

We observed another image contrast mechanism with the sample at high temperature. During annealing at ~1100°C, the image of the Ti silicide islands could be obtained without the UV-light. Furthermore, the overall brightness of the image was enhanced with increasing temperature (compare Fig. 1 with Fig. 5). A sample heated to a sufficient temperature will emit thermionic electrons. These electrons will also be imaged in the PEEM. Thus, strictly speaking. PEEM over a range of temperatures utilizes the processes of both photoemission and thermionic electron emission.

DISCUSSION

Consider the growth processes of Ti silicide islands at high temperature (Fig. 1). Previous studies have explained the island formation in terms of the surface and interface energies of the structures [4-6]. Here we suggest two possibilities to account for the increasing size of the islands and the decreasing density obtained at the higher temperature annealing. One growth process is island coalescence (the circle in Fig. 1 (b)-(e)). After the islands are grown epitaxially (facetted islands) by annealing at high temperature, substantial thermal energy could allow the islands to diffuse on the surface. Finally, the islands grow together upon when they come into close proximity. The other growth process is island ripening (the triangle in Fig. 1 (c)-(f)). It is characterized by a local interaction between two neighboring islands of slightly different size. Thermodynamically each island grows and disintegrates with the same probability. Due to the difference in island circumference, the larger islands grow at the expense of smaller islands. Both growth processes may reduce the surface-to-volume ratio of the employed system and result in a minimization of the total surface energy.

For the case of continuous deposition of Ti at high temperature (Fig. 5), we observed another mechanism of island formation. At the earliest stages, Ti silicide island initiation is a spatially random process. The spatial distance between the islands is too far to interact by the island-induced strain fields. Further deposition results in strain field overlapping caused by the dense and large islands. The adatoms on surface between the islands are preferentially adsorbed by larger islands. Furthermore, at the late stages, continued deposition allows the islands to grow together. This is another coalescence mechanism of island growth. The islands remain relatively

in place because of the lower temperature. However, with continuing deposition these islands grow larger at the perimeter of the islands. The islands coalesce when their perimeter lines touch each other and grow together. This process of coalescence can be referred to as static coalescence, compared with the dynamic coalescence process of the high temperature annealed samples [7].

Small islands (~30nm diameter) were not observed, even though our PEEM instrument has a high resolution capability of ~10nm. Regardless of the aberration of lens, the image resolution is limited by the emission current density. The emission current density depends upon the quantum efficiency (emitted electrons per incident photons) of the surface and the photon flux density of light source. We can estimate the photon flux and the current density required for imaging an island of ~ 10nm. A current density of > 1.6×10^{-4} A/cm^2 is required to observe the islands of ~10nm. Given a quantum efficiency of ~ 10^{-6} range as an average of many materials (pure metal : > 10^{-5}), the desired photon flux could be ~10^{21} photons/sec·cm^2. The photon flux of the Hg discharge lamp is several orders of magnitude lower than this(~10^{14} photons/ sec·cm^2). Therefore, a higher intensity UV source will improve the imaging of smaller islands. Secondarily, chromatic aberration, which is caused from a spread in the velocity of the emission electron, blurs the image resolution. If a photon source with a small energy spread would be tuned to just above the work function of Ti silicide (~4.6eV), better image contrast of the Ti silicide islands should be achieved. If we can use an intense tunable light source with a narrow energy distribution, we may observe small Ti silicide island formation and dynamics. In the future, as we combine our PEEM with the UV-FEL at Duke University for a light source (the photon flux: >10^{25}/sec·cm^2, energy range: 3-10eV, energy resolution: $\Delta E/E > 10^{-4}$), we anticipate real time imaging of surface Dynamics at the 10nm resolution limit of the PEEM.

CONCLUSION

In this study, we have used PEEM to observe the formation and real-time dynamics of Ti silicide islands on Si (001). Similar sized and relatively uniformly separated islands were observed for Ti deposition followed by annealing or Ti deposition at high temperature. Both growth processes of coalescence and ripening contribute to large island growth for high temperature annealing. For continuous deposition of Ti, the island growth process is characterized as static coalescence. In the future, PEEM combined with a high intensity and tunable UV-FEL should promise observation of small island formation (~10nm) and real time surface dynamics.

ACKNOWLEDGEMENTS

We gratefully acknowledge the support of T. Franz and C. Koziol from Elmitech, and P. Goeller for helpful discussions. This work was supported in part by the NSF under grant DMR 9633547 and the ONR through grant N00014-95-1-1141.

REFERENCE

[1] H. Rotermund, S. Nettesheim, A. von Oertzen and G. Ertl, Surf. Sci. Lett. **275**, L645 (1992)

[2] M. Mundschau and E. Bauer, J. Appl. Phys. **65**(2), 581 (1988)

[3] M. Giesen, R. Phaneuf, E. Williams, T. Einstein and H. Ibach, Appl. Phys. **A64**, 423 (1997)

[4] W. Yang, F. Jedema, H. Ade, R.J. Nemanich, thin solid films **308-309**, 627(1997).

[5] W. Yang, F. Jedema, H. Ade, R.J. Nemanich, Mat. Res. Soc. Symp. Proc. Vol **448**, 223(1997).

[6] H. Jeon, C.A. Sukow, J.W. Honeycutt, G.A. Rozgonyi, and R.J. Nemanich, J. Appl. Phys. **71**, 4269(1992)

[7] M. Zinke-Allmang, L. Feldman and M. Grabow, Surf. Sci. Rep. **16**, 377(1992)

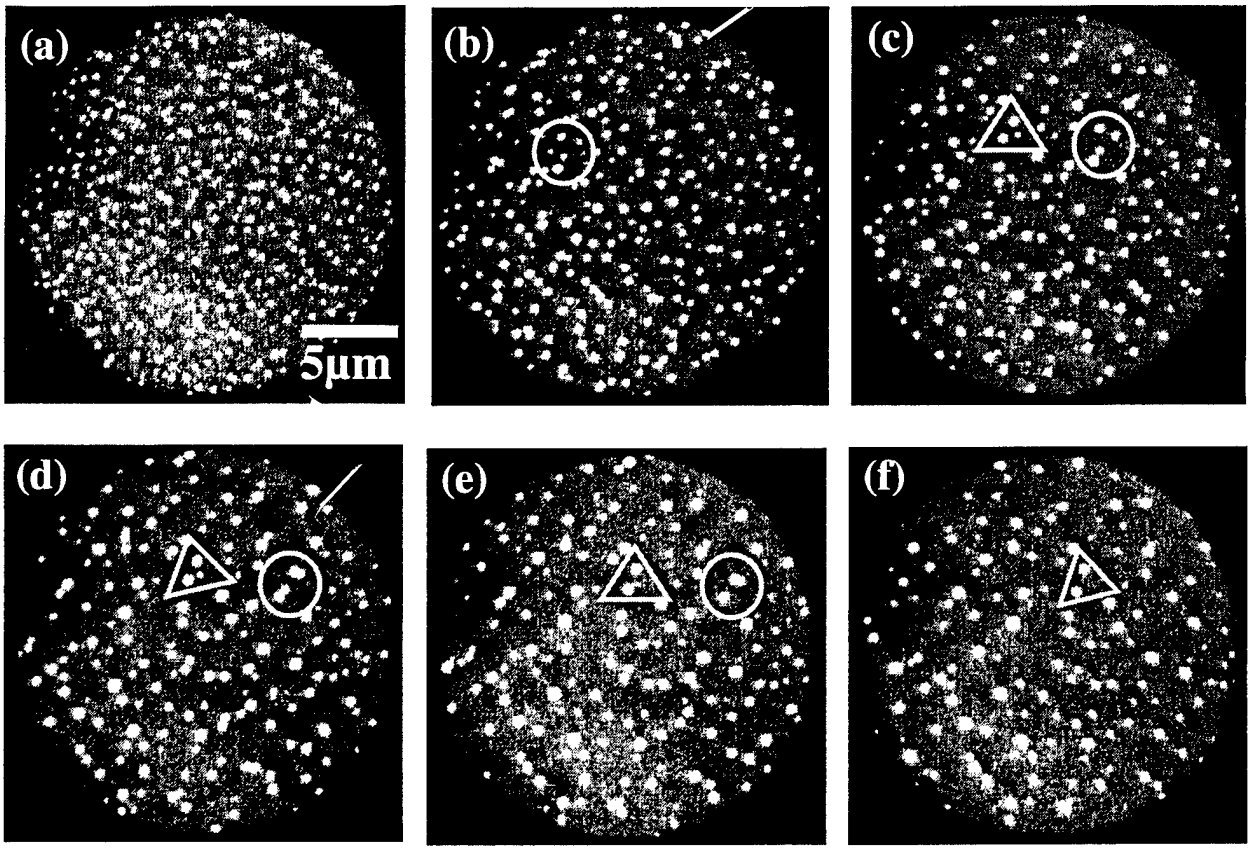

Fig. 1 PEEM images of 10ML Ti deposition followed by annealing at 1150°C for (a) 1min (b) 5min (c) 9 min (d) 10min (e) 11min (f) 15min. The islands (in the circle) coalesce and grow larger. The field of view of each image is 20μm. All images were obtained in situ, real time with the sample at the annealing temperature. The image shift is due to specimen drift at the elevated temperature.

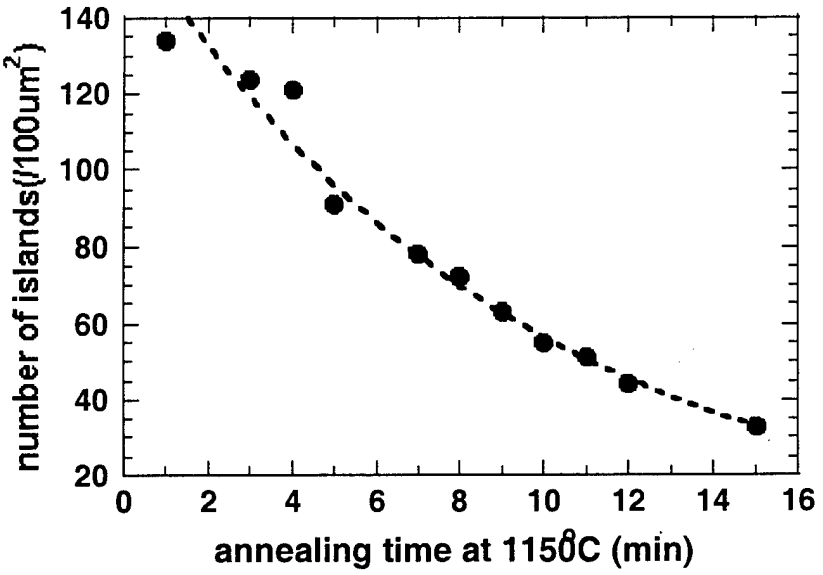

Fig. 2 The number density of islands observed at 1150°C as a function of annealing time

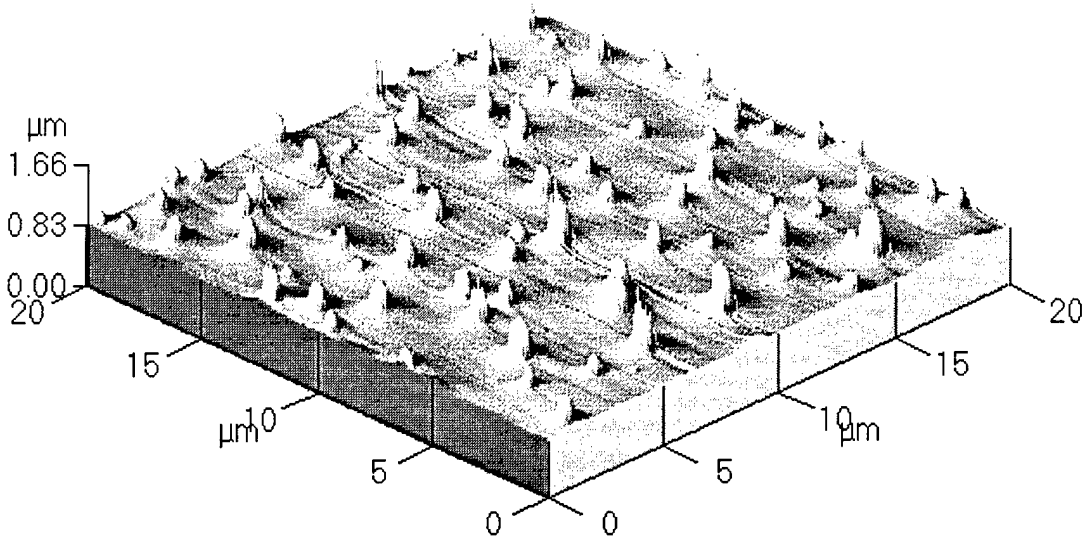

Fig. 3 A 20 x 20 μm^2 AFM 3D-rending image of 10ML Ti deposition, annealed at 1150°C

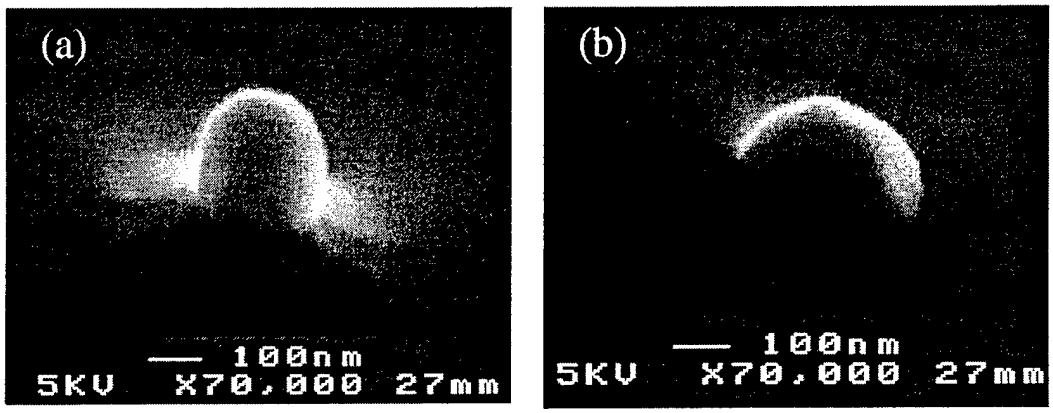

Fig. 4 SEM micrographs of $TiSi_2$ islands, showing the different shape and size of island. The sample was tilted 60° with respect to horizon.

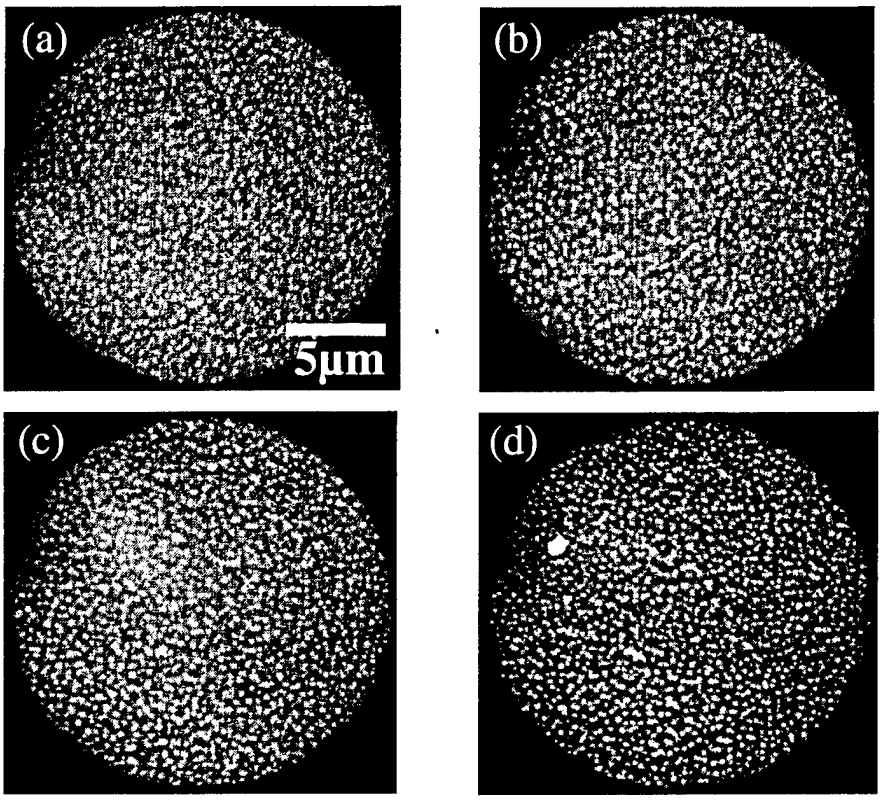

Fig. 5 PEEM images of Ti silicide islands formed with continuing deposition at 950°C. Ti deposition thickness is 3, 6, 9, 12ML for (a) through (d), respectively. All images were obtained after cooling down at room temperature. Field of view of image is 20μm.

Distribution List	Number of Copies
Program Manager/Officer ONR: 312 Larry R. Cooper Office of Naval Research Ballston Tower One 800 North Quincy Street Arlington, Virginia 22217-5660	3
Administrative Grants Officer Office of Naval Research Regional Office Atlanta 100 Alabama Street NW, Suite 4R15 Atlanta, GA 30303-3104	1
DIRECTOR, Naval Research Laboratory ATTN: Code 5227 4555 Overlook Drive Washington, DC 20375-5326	1
Defense Technical Information Center 8725 John J. Kingman Rd, Ste 0944 Ft. Belvoir, VA 22060-6218	2
Office of Naval Research ATTN: ONR 00CC1 Ballston Center Tower One 800 North Quincy Street Arlington, Virginia 22217-5660	1